Wind and Structures, *Vol. 24, No. 6 (2017) 613-635*
DOI: https://doi.org/10.12989/was.2017.24.6.613

Characteristics of downslope winds in the Liguria Region

Massimiliano Burlando*, Marco Tizzi[a] and Giovanni Solari[b]

Department of Civil, Chemical, and Environmental Engineering, University of Genoa, via Montallegro 1, 16145 Genoa, Italy

(Received March 22, 2017, Revised April 8, 2017, Accepted April 15, 2017)

Abstract. Strong downslope windstorms often occur in the Liguria Region. This part of North-Western Italy is characterised by an almost continuous mountain range along its West-East axis consisting of Maritime Alps and Apennines, which separate the Padan Plain to the North from the Mediterranean Sea to the South. Along this mountain range many valleys occur, frequently perpendicular to the mountain range axis, where strong gap flows sometimes develop from the top of the mountains ridge to the sea. In the framework of the European projects "Wind and Ports" and "Wind, Ports, and Sea", an anemometric monitoring network made up of 15 (ultra)sonic anemometric stations and 2 LiDARs has been realised in the three main commercial ports of Liguria. Thanks to this network two investigations are herein carried out. First, the wind climatology and the main statistical parameters of one Liguria valley have been studied through the analysis of the measurements taken along a period of 4 years by the anemometer placed at its southern exit. Then, the main characteristics of two strong gap flows that occurred in two distinct valley of Liguria are examined. Both these studies focus, on the one hand, on the climatological and meteorological characterisation of the downslope wind events and, on the other hand, on their most relevant quantities that can affect wind engineering problems.

Keywords: downslope winds; Alps and Apennines; (ultra)sonic anemometric measurements; LiDAR measurements; Liguria Region

1. Introduction

Severe downslope winds sometimes occur in the lee of high ridges as a consequence of internal gravity waves developing in a stably-stratified atmosphere, initiated when air is forced up the mountains and propagates downstream. After the pioneering studies carried out by Defant (1951) and Corby (1954), one of the first modern attempts to describe this kind of phenomena is reported by Klemp and Lilly (1975), who used a research aircraft to investigate the structure of the large amplitude mountain waves in the lee of the Rocky Mountains that triggered a strong downslope windstorm on January 11, 1972 in Boulder, Colorado. Since then, the basic dynamics of mountain waves and downslope winds has been clarified in some famous papers (Clark and Peltier 1977, Smith 1979, Peltier and Clark 1979, Smith 1985, Durran 1990) and sound experiments (Lilly 1978,

*Corresponding author, Professor, E-mail: massimiliano.burlando@unige.it
[a] Ph.D., PostDoc Researcher, Email: marco.tizzi@unige.it
[b] Professor, Email: giovanni.solari@unige.it

http://www.techno-press.org/?journal=was&subpage=8 ISSN: 1226-6116 (Print), 1598-6225 (Online)

Smith 1987, Meyers *et al*. 2003, Grubisic and Lewis 2004, Bond *et al*. 2006). The development of strong downslope winds, however, is not determined by mountain-induced gravitational oscillations only. The presence of cold air pools in the lee side of ridges has been demonstrated to prevent the downslope wind to reach the surface (Lee *et al.* 1989, Xu *et al.* 1996), whereas mountain gaps are able to enhance the low-level flow convergence because of the high pressure difference that occurs across the mountain ridge (Zangl 2002, Whiteman and Zhong 2008). Besides, specific meteorological contributors at the synoptic and meso-scale are usually needed as precursors to strong downslope winds as shown for instance by Romanić *et al*. (2016a) for the Koshava winds development in the Eastern Europe.

Downslope flows are observed all over the world, and strong downslope windstorms often occur in some specific areas of the Alps, as well (see for example Fig. 10.23 in Whiteman, 2000). Smith *et al.* (2007), for instance, analysed comparatively seven gravity wave cases that occurred at a finer scale in different parts of the Alps in 1999, during the special observing period of the Mesoscale Alpine Project (Bougeault *et al*. 2001). None of them, however, occurred over the Liguria Region. Nevertheless, a special kind of downslope winds, called gap winds, quite often occur along the main valleys of Liguria, especially when the air to the North of the Maritime Alps and Apennines gets to the top of the mountains and flows down the sloping surfaces towards the sea because it is cooler and denser than the maritime air standing above the warmer Mediterranean water. Following the definition of Zangl (2002), these gap flows are strong gusty winds restricted in the lee of mountain gaps or passes, with their highest speed at the valleys' exit. Their presence over the Liguria Sea is sometimes reinforced by larger scale low-pressure systems, as during secondary cyclogenesis events in the Gulf of Genoa (Trigo *et al*. 2002), so that strong and gusty slope winds can develop under particular meteorological conditions.

At the exit of some of the valleys along the Liguria coastline, anemometric measurements from (ultra)sonic anemometers and LiDAR (Light Detection And Ranging) wind profilers, installed in the framework of the European projects "Wind and Ports" (WP) 2009-2012 (Solari *et al*. 2012) and "Wind, Ports, and Sea" (WPS) 2013-2015 (Burlando *et al*. 2015), exist. In particular, there are two interesting sites where strong downslope winds frequently occur, especially in the winter season, just in the areas in which the aforementioned instruments are installed: the first one corresponds to the Vado Valley, which meets the sea in the area of the Port of Savona/Vado Ligure, where three sonic anemometers are available; the second one is the Turchino Valley, which ends in the Western part of the Port of Genoa, where one sonic anemometer and a LiDAR are installed. A brief description of the anemometric monitoring network as well as of the two sites mentioned above is reported in Section 2.

Thanks to these data the present study focuses, on the one hand, on the climatological and meteorological characterisation of the downslope winds in Liguria and, on the other hand, on the most relevant quantities that can affect wind engineering problems (i.e., mean velocities, turbulence intensities, gust factors, etc.). Accordingly, the climatology of the downslope wind events that occur in the area of the Port of Savona/Vado Ligure is first analysed in Section 3. The analysis, based on a period of 4 years, shows in particular that strong downslope windstorms occur only in the winter season. Then, two particularly strong downslope wind events in two different valleys of Liguria are investigated in Section 4. One of these events, which lasted for about 24 hours, has clearly shown a recurrence period of 11 minutes, similar to Bora in the Italian Eastern Alps. In the other event, which lasted about 12 hours, a nose-shaped profile has been detected by means of a LiDAR, with maximum velocity at 120 m above ground. Throughout the text, the authors refer from the methodological point of view to a parallel series of papers in which,

starting from the data provided by the monitoring network used herein, synoptic and non-synoptic windstorms are separated (De Gaetano *et al.* 2013) and the properties of thunderstorm outflows are investigated (Solari *et al*. 2015). Conclusions and prospects are drawn in Section 5.

2. Anemometric monitoring network

During the projects WP and WPS, 14 anemometric stations and two wind profilers have been installed in the Ports of Savona/Vado Ligure, Genoa, and La Spezia. A description of the main characteristics of these instruments is reported in Table 1. All the anemometric devices of this network are bi- or tri-axial (ultra)sonic anemometers with sampling rate 10 Hz, which makes them suitable for turbulence measurements too. The two wind profilers are WINDCUBE v2 Offshore pulsed LiDARs by Leosphere, which can measure vertical wind profiles at 12 heights above ground level from 40 m up to about 250 m, with a sampling rate of 1 Hz. A wide literature exists that testifies the accuracy of LiDAR measurements of mean wind velocity profiles (Wilczak *et al*. 1996, Smith *et al*. 2006, Pena *et al*. 2009) whereas fluctuations involve some inconsistencies (Wilczak *et al*. 1996, Sathe *et al.* 2011, Sathe and Mann 2013) and their detection is still controversial; however, it seems reasonable to expect that LiDARs may provide at least a qualitative description of the vertical variation of the ambient turbulence.

Table 1 Main characteristics of the anemometric monitoring network

Port	Instrument	Type*	Position	Height AGL (m)	Sampling rate (Hz)	Installation date**
Savona/Vado Ligure	SV.00	U3D	Building	84.0	10	2010-Q4
	SV.01	U3D	Tower	33.2	10	2010-Q4
	SV.02	U3D	Building	12.5	10	2010-Q4
	SV.03	U3D	Building	28.0	10	2010-Q4
	SV.04	U3D	Tower	32.7	10	2010-Q4
	SV.05	U3D	Tower	44.6	10	2010-Q4
	SV.51	LiDAR	Square	0.0	1	2014-Q2
Genoa	GE.02	U2D	Quay	13.3	10	2010-Q4
	GE.03	U2D	Building	32.0	10	2015-Q2
	GE.51	LiDAR	Quay	5.0	1	2015-Q2
La Spezia	SP.01	U2D	Building	15.5	10	2010-Q4
	SP.02	U2D	Tower	13.0	10	2010-Q4
	SP.03	U2D	Tower	10.0	10	2011-Q1
	SP.04	U2D	Building	11.0	10	2011-Q2
	SP.05	U2D	Dam	10.0	10	2012-Q3
	SP.06	U2D	Building	16.0	10	2015-Q1

*Instrument types are: (ultra)sonic tri-axial anemometer (U3D); (ultra)sonic bi-axial anemometer (U2D); wind profiler (LiDAR)

**Installation dates are reported in terms of quarters (Q1, Q2, Q3, Q4) of the year (YYYY).

The length of the available data sets is variable and depends on when the instruments have been installed, ranging from a maximum of about 4 years for the anemometers to about 1 year for the LiDAR in the Port of Genoa. The position of the instruments has been chosen to cover as more homogeneously as possible the port areas and, at the same time, to get undisturbed wind velocity measurements. Some anemometers are mounted on the top of buildings, at no less than 4 m above the building's roof, or on the top of lighting towers (the height of the instruments in Table 1 is above ground level, AGL). The LiDARs are positioned on the ground.

Fig. 1 shows the position of all these devices in the corresponding port areas. The Port of La Spezia is characterised by less intense downwind events, on average, with respect to the Port of Savona and Genoa, probably also because it is partially sheltered by the urban area when the wind blows from the Northern sectors. This is also true for the instruments installed in Savona (SV.00, SV.01, SV.02, SV.51) and in the Eastern part of the Port of Genoa (GE.03). The most interesting measurements are recorded in the Port of Vado Ligure (SV.03, SV.04, SV.05) and in the Western part of the Port of Genoa (GE.02, GE.51), instead.

The anemometers in Vado Ligure, shown in Fig. 2(a), are placed at the Southern exit of the valleys that from the Colle di Cadibona (436 m above sea level, ASL), which represents the break between the Ligurian Alps to the West and the Apennines to the East, extend to the Mediterranean Sea. The anemometer, GE.02, and the LiDAR, GE.51, in the Port of Genoa, are placed at the exit of the Turchino Valley to the North, as shown in Fig. 2(b). This is a valley where strong downslope winds often occur, so that these measurements are particularly interesting to analyse katabatic flows coming from the Apennines to the North-Western of the city down to the Mediterranean.

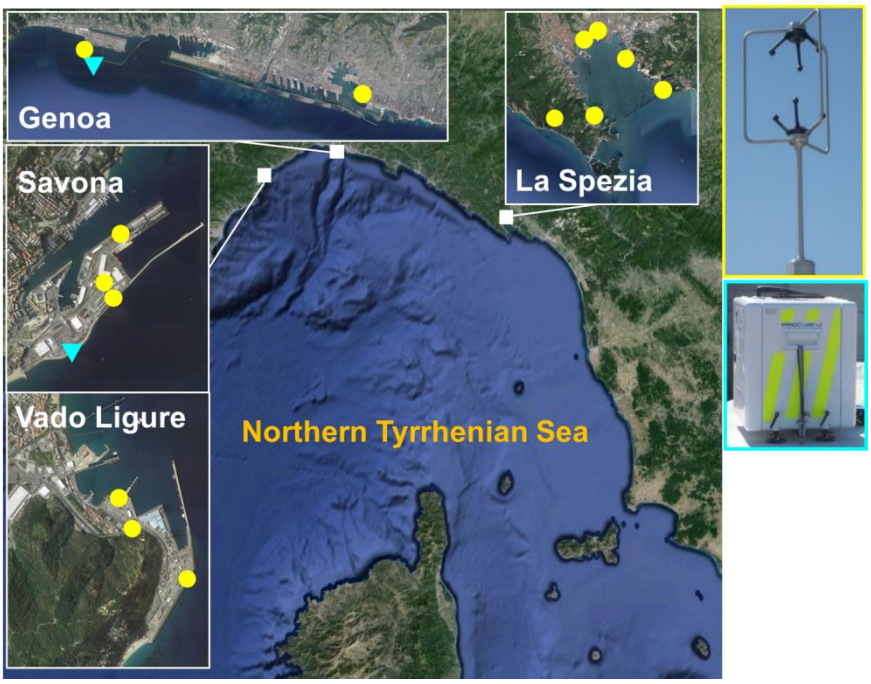

Fig. 1 Monitoring network in the Ports of Savona/Vado Ligure, Genoa, and La Spezia: anemometric stations (circles); LiDARs (triangles)

(a)

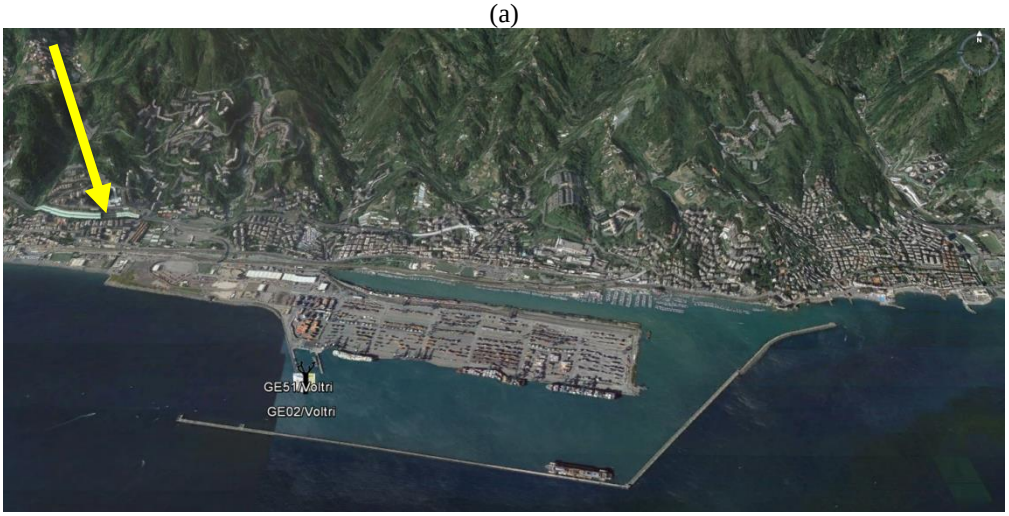

(b)

Fig. 2 Perspective view from South of the Port of Vado Ligure (a) and the western part of the Port of Genoa (b). Arrows show the two valleys connecting Colle di Cadibona (a) and Turchino Pass (b) to the Ligurian Sea

3. Statistical analysis of downslope wind events

In the present section, all the measurements recorded at the anemometer SV.04 in the Port of Vado Ligure have been analysed in order to evaluate the wind climatology of this area, with special attention to the strong winds blowing from land that may be classified as downslope windstorms.

This anemometric station, equipped by a Gill Instruments WindMaster^{TM} Pro tri-axial (ultra)sonic anemometer that can measure the wind speed from 0 to 65 m/s with a resolution of 0.01 m/s and the wind direction with the resolution of 0.1°, is placed on the top of a lighting tower

at about 33 m AGL. Raw data are stored with sampling frequency 10 Hz from the 4th quarter of 2010. However, during the first year of measurements some quite long data missing periods occurred, so that only 4 years have been considered for the present analysis, from the 22nd of October 2011 to the 21st of October 2015. All data are routinely checked for wrong values and outliers, which is particularly important for extreme distribution analysis. Table 2 provides an overview of the main characteristics of the analysed dataset. Numbers refers to 10-minute average data packets.

The probabilistic analysis of the parent population and extreme value distributions of SV.04 is illustrated in Section 3.1: the former represents the basic information for wind energy assessment (Kwon 2009), wind environmental evaluations (Lu and Fang 2002) and wind-induced fatigue analysis of steel structures (Repetto and Solari 2010); the latter is the crucial element to perform ultimate (Kareem 1990, Chen and Huang 2010) and serviceability (Pagnini and Solari 1998) limit state structural verifications. A comparison between the time series of the 4-year dataset and those of some selected strong events blowing from the valley to the North of Vado Ligure is performed in Section 3.2 in order to show the main characteristics of downslope windstorms in terms of mean values, turbulence intensities and gust factors, these being the key parameters to deal with any wind engineering problem.

3.1 Probabilistic analysis

A probabilistic analysis of the 4-year long SV.04 dataset has been carried out in order to infer the directional and non-directional distribution functions of the wind speed, $F_V(v)$, based on the hybrid Weibull distribution model (Weibull 1951, Takle and Brown 1976, Solari 1996a)

$$F_V(v) = 1 - (1 - P_0)\sum_{j=1}^{S} A_j \mathrm{e}^{-\left(\frac{\mathrm{v}}{C_j}\right)^{K_j}} \tag{1}$$

$$F_V(v) = P_0 - (1 - P_0)\left[1 - \mathrm{e}^{-\left(\frac{\mathrm{v}}{C}\right)^{K}}\right] \tag{2}$$

where P_0 is the frequency of wind calms. In the directional distribution, Eq. (1), the whole dataset is firstly subdivided into *S* subsets according to the direction sector that the wind is coming from. Then, for each *j*-th direction sector, the corresponding shape and scale model parameters, K_j and C_j, are evaluated, A_j being the frequency of occurrence. In the non-directional distribution, Eq. (2), K and C are the shape and scale model parameters of the whole dataset. In both cases the shape and scale parameters are estimated by resistant method (Hoaglin *et al*. 1981) excluding wind calms and best fitting the tail of the distribution.

Table 2 Total number and percentage of missing data, wind calms, and non-zero intensity data in the SV.04 dataset. Overall data are computed over the considered 4 years, from 2011-10-22 to 2015-10-21. Percentages of wind calms and non-zero values refer to valid data

Overall	Missing	Valid	Wind calms*	Non-zero values
210.384	25728	184656	2200	182456
100 %	12.2 %	87.8 %	1.2 %	98.8 %

*Wind calms are conventionally referred to as wind speed values smaller than 0.5 m/s

Also the probabilistic analysis of the extreme wind speed distribution, $F_M(v)$, has been performed, based on the first type and process distribution models (Gumbel 1954, Gomes and Vickery 1977, Solari 1996b)

$$F_M(v) = e^{-e^{-a(v-u)}} \tag{3}$$

$$F_M(v) = e^{-\lambda f_V(v)} \tag{4}$$

where a, u and λ are model parameters; a and u are estimated by resistant method whereas λ is determined by counting threshold up-crossings (Gomes and Vickery 1977). Eq. (4) provides a link between the wind speed extreme value distribution and density function of the parent population (Eqs. (1) and (2)). Under this point of view, it makes use of more information than Eq. (3), whose application is usually based on a limited series of maximum values, so it is appropriate also with reference to a limited number of years of data. Under this point of view it allows to perform reasonably approximated statistical analyses referred to relatively high return periods based on a limited number of years of measurements. In addition, it is normally more adherent to reality than Eq. (3) that tends to overestimates wind speed just with reference to high return periods (Lagomarsino *et al*. 1992) most crucial for structural safety analyses, and allows to easily take into account missing data. Its reliability has been recently proved by means of long-term Monte Carlo simulations of synthetic wind velocity time-series (Torrielli *et al*. 2013, 2014).

Table 3 shows the values of mean, standard deviation, shape and scale parameters of the directional and non-directional distributions evaluated by means of Eqs. (1) and (2), as well as the wind speed values corresponding to decreasing exceeding probabilities, defined as $1 - F_V(v)$. Note that rows corresponding to sectors 210°-240° and 240°-270° are empty because the frequency of occurrence, A_j, of the wind blowing from these sectors is too low in order to obtain reliable estimates of the related distribution parameters.

Fig. 3(a) shows the wind rose as calculated through the 4-year long SV.04 dataset: it represents a roughly bi-modal distribution with two main peaks centred around South and North-West. The sectors centred around NW are by far the most frequent ones, especially in winter. The highest wind speed values, i.e. greater than 15 m/s, occur mainly from S and NW. This is also confirmed by the statistical analysis depicted in Fig. 3(b), which shows the directional distributions of the wind speed corresponding to exceeding probabilities from 10^{-2} to 10^{-6}. Fig. 3(c) shows the exceeding probability corresponding to increasing wind speed values evaluated according to the directional and non-directional distribution functions defined through Eqs. (1) and (2), respectively, represented on the Weibull probability paper. Fig. 3(d) shows the wind speed values corresponding to long return periods, R, calculated using the process and asymptotic analyses, represented on the Gumbel probability paper. A correction of the results provided by the process analysis has been also performed according to Burlando *et al*. (2013) in order to account for the incompleteness of the dataset due to the presence of missing values. In this latter case the extreme wind speed corresponding to the return period of 50 years is equal to 25.2 m/s. This value agrees with the results obtained by Castino *et al*. (2003), who performed a high-resolution evaluation of the wind climate all over the Liguria Region. The corresponding extreme wind speed as evaluated by Eurocode 1 (2005) and the Italian Guide for the assessment of wind actions and effects on structures (CNR-DT 207/2008, 2010), equal to 26.3 m/s, is slightly higher than the present one.

Table 3 Directional (based on 30°-wide sectors) and non-directional analysis of the wind speed distributions calculated through Eqs. (1) and (2). The overall frequency A, reported in the last row, is smaller than 1 because wind calms are not considered

Sector	Mean (m/s)	StDev (m/s)	A	K	C (m/s)
0-30	3.418	2.312	0.0223	1.407	3.263
30-60	3.558	1.951	0.0311	1.774	3.508
60-90	3.049	1.507	0.0356	1.590	2.757
90-120	3.128	1.672	0.0444	1.363	2.685
120-150	3.594	2.024	0.0593	1.309	3.125
150-180	4.572	2.590	0.1091	1.284	4.246
180-210	5.224	3.188	0.0586	1.517	5.251
210-240	-	-	0.0057	-	-
240-270	-	-	0.0030	-	-
270-300	4.377	2.221	0.0593	1.842	4.330
300-330	5.541	2.680	0.4768	1.829	5.590
330-360	5.435	3.199	0.0829	1.775	5.600
0-360	4.820	2.770	0.9881	1.561	4.818

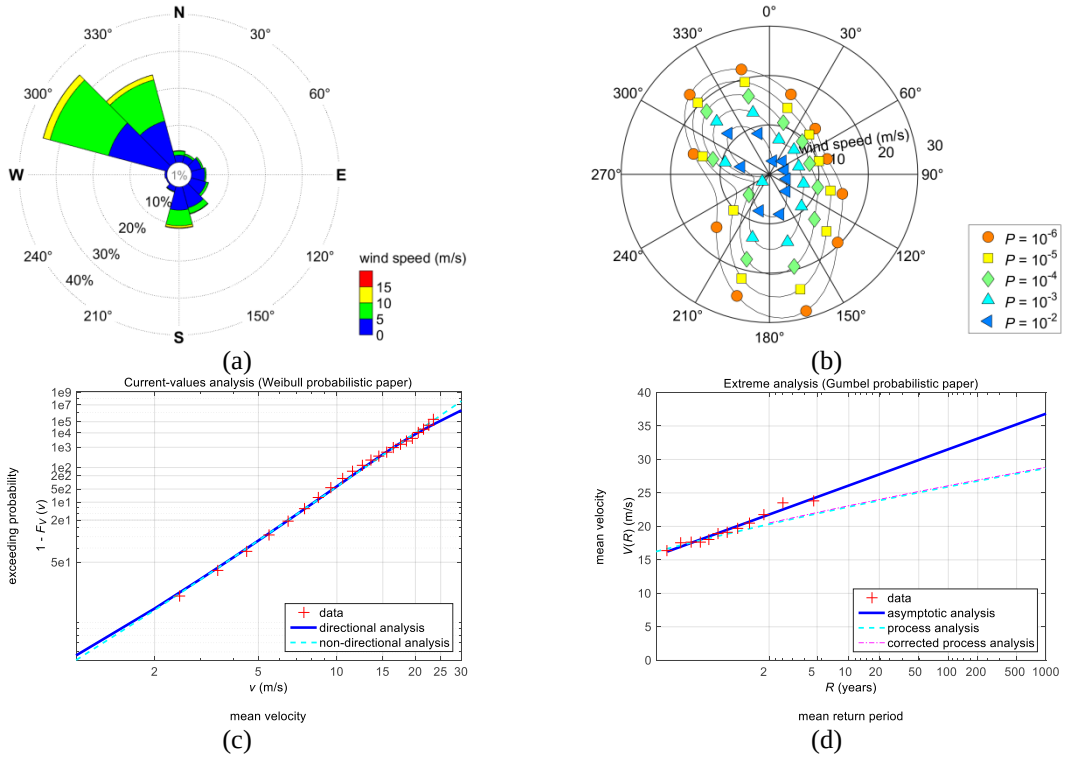

Fig. 3 Wind rose (a), directional and non-directional wind speed distributions corresponding to decreasing exceeding probability values (b)-(c), and extreme wind speed values for different return periods (d) for the 4-year long dataset SV.04

3.2 Time series analysis

In the present section, a time series analysis is presented in order to investigate the behaviour of mean wind velocity and turbulence when downslope windstorms occur. The time series considered are the 10-minute averaged wind speed, $\bar{v}$, and direction, θ, values, the peak wind speed, $\hat{v}$ defined as the maximum 1-second averaged wind speed, the longitudinal turbulence intensity, $I_v = \sigma_v/\bar{v}$, where σ_v is the standard deviation, and the gust factor, $Gv = \hat{v}/\bar{v}$.

Fig. 4(a) shows the 4-year long time series of the 10-minute average wind speed and direction measured at the anemometric station SV.04, as well as the peak wind speed recorded every 10 minutes. Data corresponding to the wind blowing from the fourth quadrant, i.e., from 270° to 360°, which are the directions that the valley winds belong to (see Fig. 2), are coloured darker. All the other quadrants, which correspond to the wind blowing from the sea, are coloured lighter. The mean wind speed only occasionally exceeds 20 m/s, while values higher than 15 m/s often occur. The peak wind speed often exceeds 20 m/s and it is higher than 30 m/s in a few events. It is worth noting that, despite the greater roughness of the up-wind terrain, on average, mean and peak wind speed values are higher when the wind blows from land than from sea. The occurrence of high mean wind speed values related to rough terrains, and thus large turbulent fluctuations too, tends to produce relevant wind loading on structures.

A subset of the whole SV.04 dataset corresponding to the strongest events selected according to the criterion that $\bar{v} > \bar{v}^{P99}$, where $\bar{v}^{P99} = 12.59$ m/s is the wind speed of the 99th percentile of the population distribution, is reported in Fig. 4(b). It is shown that the strongest events in Vado Ligure correspond to the wind blowing from the fourth quadrant (darker symbols) and to the wind blowing from South (lighter symbols). This result can be extended to the whole Liguria Region: as a general rule, in Liguria the strongest surface wind conditions occur during downslope wind events or sea storms. Downslope winds, in particular, occur mainly in the winter season with higher frequencies of occurrence in November and February-March. They occur with the same frequency during day and night, instead.

Downslope winds and sea storms have quite different behaviours in terms of turbulence intensity and gust factors. During sea storms the higher mean values correspond quite regularly to higher peak values, and gust factors are almost always lower than 1.5, as it is typical of neutral atmospheric stratification and smooth terrain. This is not the case during downslope winds, where turbulence intensity is, on average, higher than during sea storms whereas gust factors between 1.5 and 2.0 usually occur and sometimes also exceed the value 2; these values are considerably higher than those commonly experienced in neutral atmospheric stratification and rough terrain. Such differences cannot be explained only in relation to the different roughness of the upwind terrain (Engineering Sciences Data Unit, 1993), using the classical wind engineering hypothesis that intense wind speeds are related to neutral atmospheric stratifications.

Fig. 5 clarifies these remarks showing the longitudinal turbulence intensity (Fig. 5(a)) and the gust factor (Fig. 5(b)) as functions of the mean wind speed when the wind blows from land ($270° < \alpha < 360°$) and sea ($\alpha < 270°$) with darker and lighter symbols, respectively.

Fig. 5(a) shows that, when the mean wind speed is low, e.g. $\bar{v} < 5$ m/s, the turbulence intensity values are highly dispersed because of atmospheric stability conditions far from neutral. Note, however, that I_v values much greater than 1 can be spurious values that occur when $\bar{v}$ is close to 0. For higher mean wind speeds, e.g., $\bar{v} > 10$ m/s, instead, turbulence intensity approaches an asymptotic value which is roughly 0.2 for the north-western sectors, and 0.1 for the other directions (see the darker dashed and the lighter solid lines in Fig. 5(a)).

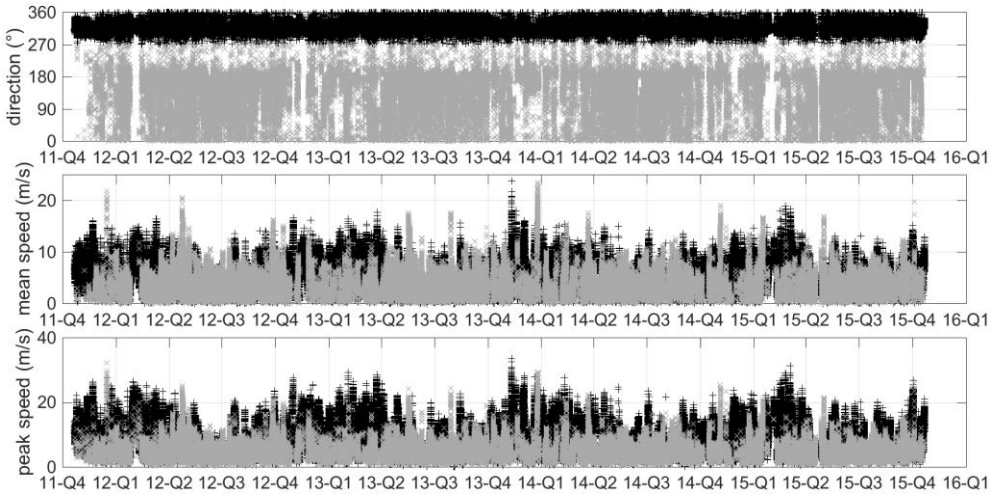

(a)

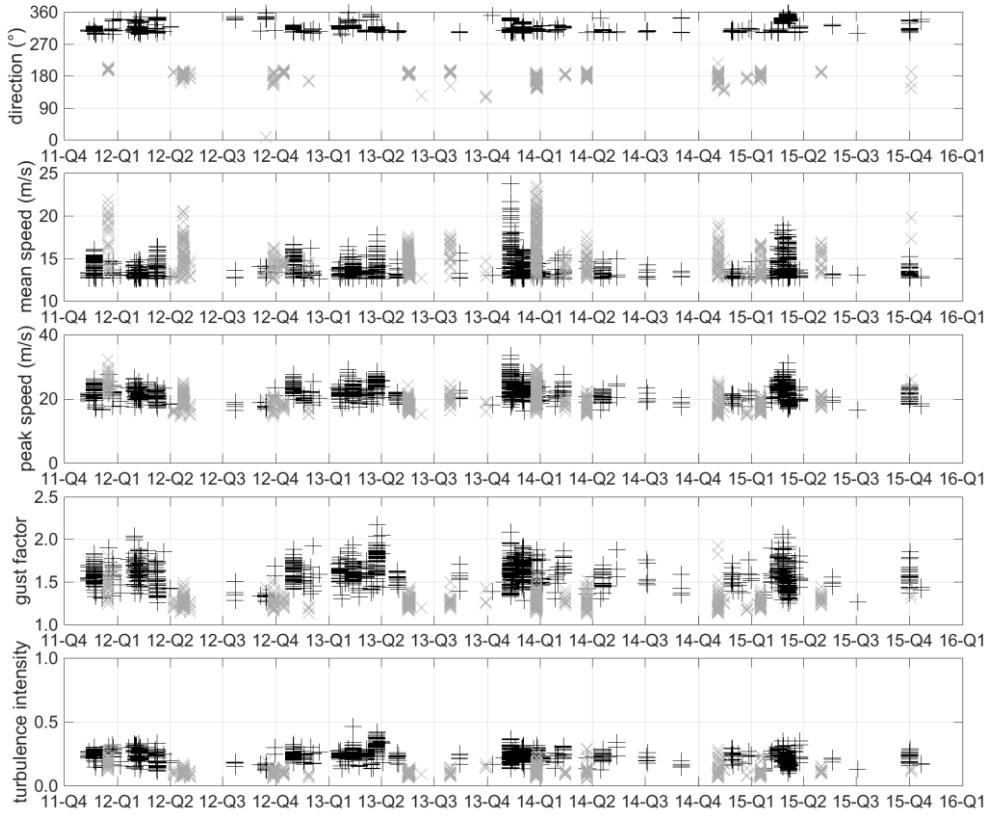

(b)

Fig. 4 Time series of mean wind speed and direction, and peak wind speed of the 4-year long dataset SV.04 (a); and mean wind speed and direction, peak values, gust factors, and longitudinal turbulence intensity of the strongest wind events recorded at SV.04 (b)

A very similar behaviour has been also reported by Pagnini *et al*. (2015), who have analysed the dataset SV.02 placed in the Port of Savona. According to the asymptotic turbulence intensity values, equivalent roughness lengths can be evaluated through the approximate formula provided for instance by Eurocode 1 (2005) and CNR-DT 207/2008 (2010), assuming neutral atmospheric conditions

$$I_v = \frac{1}{\ln(z/z_0)} \tag{5}$$

where $z = 32.7$ m is the SV.04 anemometer's height AGL, as reported in Table 1, and z_0 is the roughness length. Inverting Eq. (5) based upon the two estimates of the asymptotic turbulence intensity values, I_v = 0.2 and 0.1, one obtains the equivalent roughness $z_0 \cong 0.0015$ m for sea storms and $z_0 \cong 0.22$ m for downslope windstorms. Both these values match rather closely the typical values commonly attributed to rough terrains and sea exposure.

Fig. 5(b), referred to the gust factor, shows a trend qualitatively similar to Fig. 5(a), related to turbulence intensity, but even more pronounced. Starting from the two asymptotic estimates of the equivalent roughness $z_0 \cong 0.0015$ m for sea storms and $z_0 \cong 0.22$ m for downslope windstorms, and using the method proposed by Solari (1993) for intense wind speeds and neutral atmospheric conditions, the gust factor is almost independent of the mean wind speed and assumes the values 1.57 for the north-western sectors, and 1.29 for the other directions (see the darker dashed and the lighter solid lines in Fig. 5(b)). However, while the trend exhibited by G_v for sea winds, like that shown by I_v, is perfectly coherent with typical measurements in smooth terrain, the spread of G_v for the downslope winds, much more than the one of I_v, points out conditions that suggest the occurrence of different wind phenomena, e.g., synoptic depressions and thermal winds, characterised by different properties. Moreover, the occurrence of very large values of G_v also with reference to intense wind speeds suggests the existence of phenomena, other than synoptic depressions, for which intense wind speeds may be associated also to non-neutral atmospheric conditions (Romanić *et al.* 2016b, Sterling *et al*. 2006).

This matter clearly deserves further investigations especially with reference to the modern trend in wind engineering aiming to deal with mixed wind climate conditions by separating different aeolian phenomena (Lombardo *et al*. 2009, Kruger *et al*. 2012, De Gaetano *et al.* 2014) in order to determine refined wind speed statistics (Gomes and Vickery 1977/1978, Harris and Cook 2014), wind loading and structural response (Solari 2014).

4. Analysis of two strong downslope wind events

In the following sections, two strong downslope wind events are described and analysed. The first event, reported in Section 4.1, corresponds to the strongest downslope wind measured at the anemometric station SV.04 in the Port of Vado Ligure (see Fig. 3), which occurred on November 11, 2013 at 03:00 UTC. The second event selected, reported in Section 4.2, corresponds to a strong downslope wind measured by means of the LiDAR GE.51 installed in the western part of the Port of Genoa. LiDAR measurements provide information up to 250 m AGL, which is particularly interesting as it allows to analyse the wind profile of the whole atmospheric surface boundary layer.

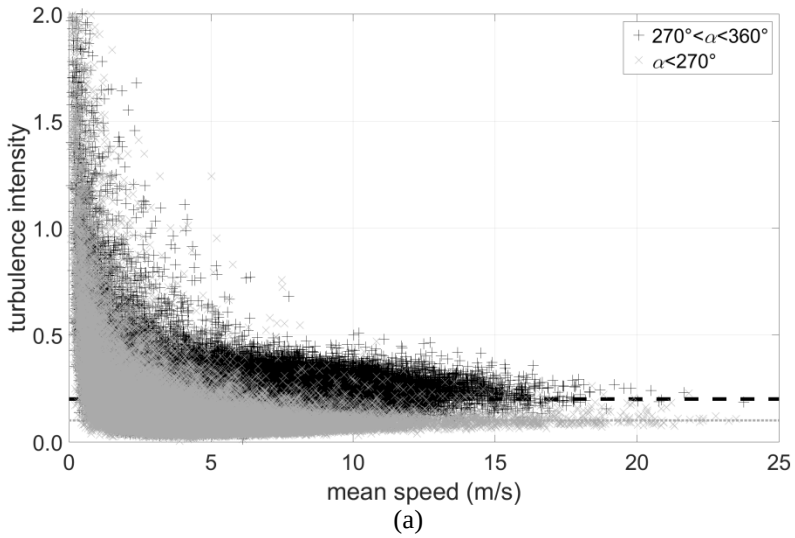

(a)

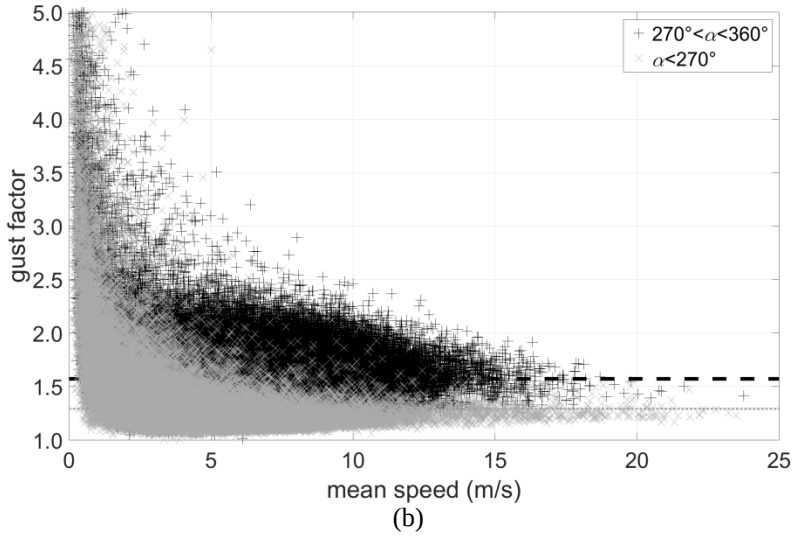

(b)

Fig. 5 Longitudinal turbulence intensity (a) and gust factor (b) as function of mean wind speed for the 4-year long dataset SV.04. The darker dashed line and the lighter solid line in (a) correspond to the asymptotic turbulence intensities 0.25 and 0.1, respectively. The darker dashed line and the lighter solid line in (b) correspond to the asymptotic gust factors 1.72 and 1.29, respectively.

4.1 The event of November 11, 2013 in Vado Ligure

On the November 11, 2013, during the night, the European scenario was dominated by a tropopause anomaly cut-off located over the Tyrrhenian Sea, coupled with a frontal system with surface low located on Southern Italy, and by a large high-pressure area over North-western Europe. Thus, the jet stream flew southwards over the Western Alps and Ligurian Sea and a strong

meridian gradient occurred between Northern France and Southern Italy. On a local scale, this configuration implied the presence of a strong low level jet crossing the Western Ligurian Apennines, flowing through its lowest passes, such as the Cadibona Pass, just North of Vado Ligure.

This meteorological condition is depicted in Fig. 6, which shows the cloud top height obtained from the cloud analysis performed by Eumetsat (Eumetsat 2013, NWC SAF 2013) based on infra-red measurements collected by SEVIRI (Spinning Enhanced Visible & Infrared Imager) on board Meteosat Second Generation satellites. From the cloud cover, the cyclonic rotation over the Tyrrhenian Sea is clearly visible, as well as the clear sky conditions that occur all over the Central and Western Liguria. This implies that the event recorded on November 11, 2013 in Vado Ligure was due to a strong cold advection at any level that affected the entire North-western Italy for about 24 hours.

The time series of 10-minute average wind speed and direction, peak wind speeds, gust factors and longitudinal turbulence intensity recorded at SV.04 the 11 November 2013 are shown in Fig. 7. This strong downslope winds started blowing after 18:00 UTC the day before and lasted about 24 hours. During this period the mean wind speeds are often greater than 15 m/s, the peak wind speed values reach 30 m/s, which determine gust factors up to 2, and the longitudinal turbulence intensities vary around 0.25. Note that this value fits the asymptotic turbulence intensity behaviour shown in Fig. 4 for the wind blowing from North-West.

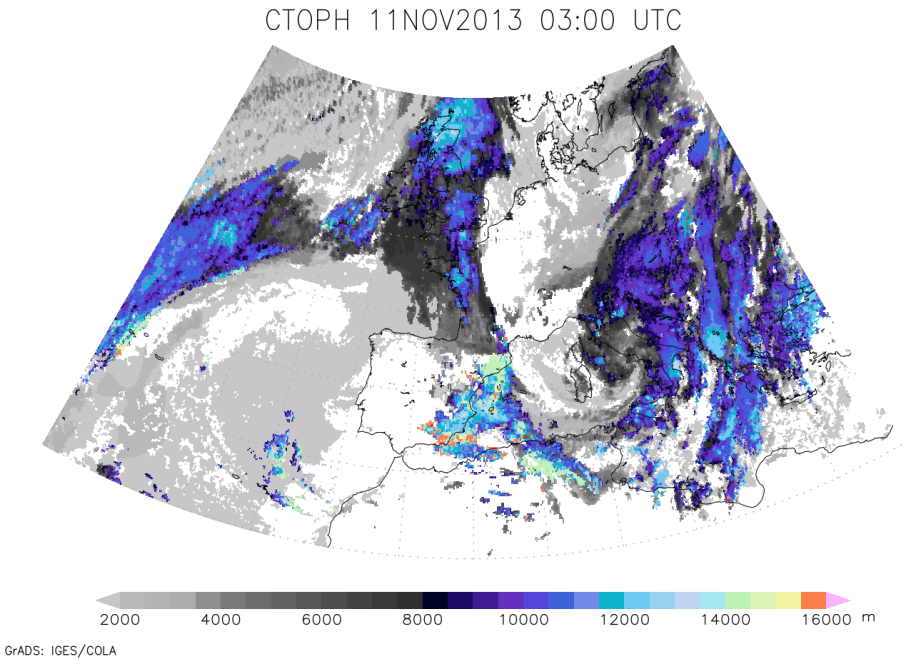

Fig. 6 Satellite image of the cloud top height (metres ASL) over the Western Europe valid for November 11, 2013 at 03:00 UTC

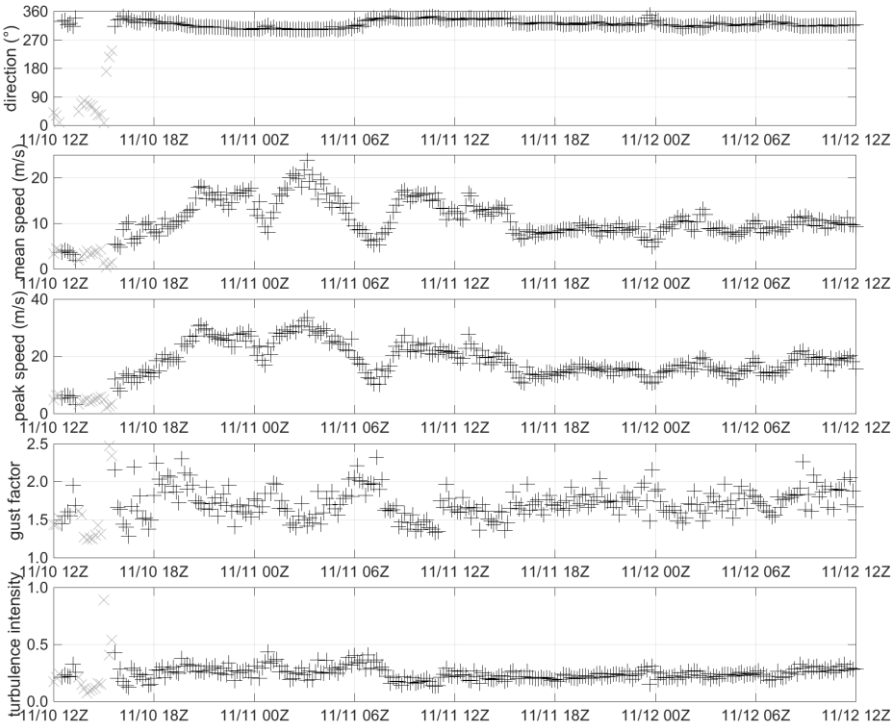

Fig. 7 Time series of mean wind speed and direction, maxima, gust factors, and longitudinal turbulence intensity of the event recorded on November 11, 2013 at SV.04. Plus symbols correspond to the wind blowing from the fourth quadrant

During the downslope wind event reported in Fig. 7, the time series of mean and peak wind speed seem to have some regular periodicities that could be worth analysing. For this reason, the spectral content of the 24-hour time series (from 18 UTC November 10 to 18 UTC November 11) of raw wind speed data, i.e., recorded at 10 Hz, of SV.04 has been analysed through a Fast Fourier transform, shown in Fig. 8. It is worth noting that some non-negligible peaks occur in the region of the spectral gap, i.e. between 10 minutes and 1 hour, for example at about 3.0×10^{-4} and 5.5×10^{-4} Hz, which correspond to 1 hour and 30 minutes, respectively. The highest peak in the spectral gap, however, is the one indicated by means of the black arrow in Fig. 8, which occurs at about 1.5×10^{-3} Hz, corresponding to approximately 11 minutes. A first attempt to explain regularities in gustiness, firstly observed during the severe downslope windstorm of January 11, 1972 in the Eastern slope of Rocky Mountains by Lilly and Zipser (1972), is reported by Clark and Farley (1984), who suggested a possible mechanism based on the competition between mountain gravity wave build up and convective wave breakdown. Pulsations of this order of magnitude have been reported in many experimental observations, like in Neiman *et al.* (1988), who detected spectral peaks at about 4-5 and 14-minute time scales, or more recently in Belusic *et al*. (2004, 2007) during Bora downslope windstorms in the Dinaric Alps, who measured pulsations in the range between approximately 3 and 11 minutes. These authors noticed a relation between

quasi-periodic gust behaviour and decrease in the upper-tropospheric jet stream, supported by surface measurements and radiosonde data comparison.

Katabatic winds, defined as local downslope gravity flows caused by nocturnal radiative cooling near the surface under calm clear-sky conditions (Barry 1992), have also been noticed to show pulsations. Van Gorsel *et al.* (2003), for instance, measured velocity oscillations in katabatic flows inside the Riviera Valley (Swiss) with period of 18 minutes, which they explained through the theory of compression warming (Fleagle 1950). However, they also measured oscillations of the wind direction, i.e., from downslope to upslope, which have not been observed in our measurements, so that the physical reason for their oscillation is probably different from the event in Vado Ligure. A somewhat different behaviour, from the one reported by Van Gorsel et al., has been observed by other authors during night-time katabatic flow events: Doran and Horst (1981) measured oscillations with average period of about 1.5 h; Bastin and Drobinski (2005) reported oscillation periods between 1 h and 1.5 h; Princevac *et al*. (2008) found oscillations with pulsation periods of 55 min and 110 min. In these cases, which show pulsation periods of the same order of magnitude, the variability of the oscillation frequency seems to be due to slightly different stability conditions of the atmosphere.

All these values, however, are quite different from the main pulsation period measured during the downslope event of November 11, 2013 in Vado Ligure. Moreover, the event in Vado Ligure lasted 24 hours, whereas the katabatic flows mentioned above typically occur during night time only. This suggests a somewhat different dynamical mechanism for oscillation excitation, which could be correlated to larger-scale forcing periodicities as well. However, the exact meteorological reason of such gustiness pulsation and its potential effects in the context of wind engineering require further investigations, possibly making use of high-resolution meso-scale meteorological models to provide information about the overall atmospheric conditions in space and their evolution in time.

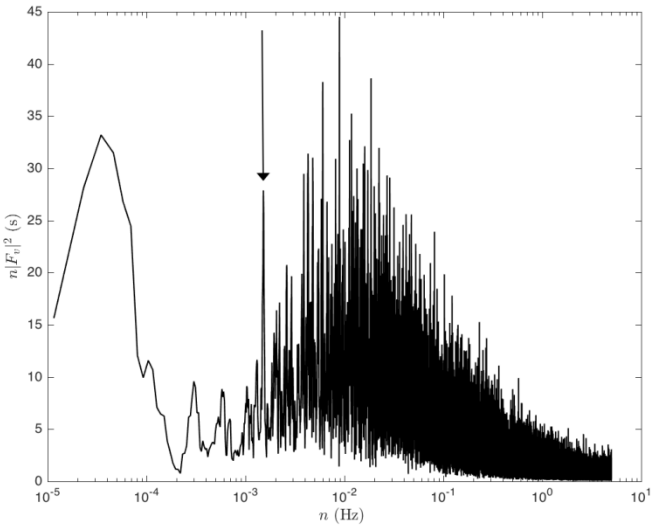

Fig. 8 Spectrum of the 24-hour long downslope wind event that occurred from 18 UTC Nov 10 to 18 UTC Nov 11, 2013 at SV.04

4.2 The event of November 2, 2015 in Genoa

A synoptic configuration rather different from the one presented in Section 4.1 characterized Europe on November 2, 2015, as shown in Fig. 9: on the one hand, a large anticyclonic ridge spread out over the European continent from the African coast up to Scandinavia with its centre of mass localized in the Balkan region, which leaded clear sky conditions all over this area; on the other hand, a deep Atlantic depression was hitting the Iberian Peninsula, where medium and high clouds occurred. The resulting temperature and pressure gradient leaded to north-easterly winds blowing over Northern Italy from the Adriatic Sea, filling the Po Valley with cold air.

Furthermore, the clear sky contributed to a strong air cooling due to night radiation, increasing the surface pressure field up to a local maximum in the Padan Plain. Strong northerly winds were triggered over Liguria when this "cold cushion" started to overflow through Apennines passes, such as the Turchino Pass. The air over the Mediterranean Sea, however, did not cool as much as over the Padan Plain because of the upward sensible heat flux caused by the higher sea surface temperature that, in November 2015, was slightly less than 20℃ along the Ligurian coast (the buoy closest to Genoa, placed in the Western part of Liguria, measured 19.8℃ on October 20, 2015). At 07 UTC, the temperature measured at the Turchino Pass (590 m ASL) was 5.4℃, the one measured along the Turchino Valley (270 m ASL) was 8.6℃, and the one measured at the Southern exit of the valley (104 m ASL) was 11.7℃. At the same time, the temperature measured 6 km eastward of the valley's exit at 69 m ASL was 14.7℃. This is 2.7℃ higher than expected by dry adiabatic warming. Note that the temperature at the exit of the Turchino Valley was 1.4℃ higher than expected also, while the temperature measured along the valley perfectly corresponds to the adiabatic warming. This behaviour seems to be coherent with the hypothesis of a gap flow influenced by the presence of a warm pool downstream of the mountain barrier.

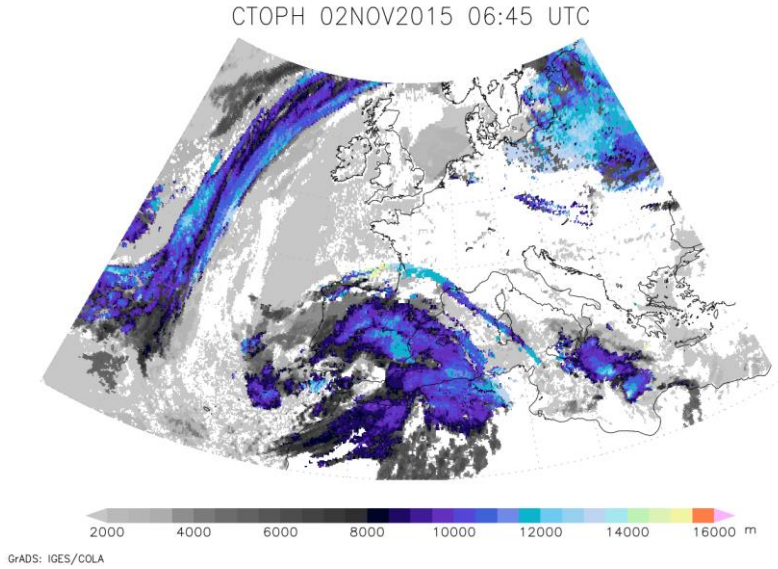

Fig. 9 Satellite image of the cloud top height (metres ASL) over the Western Europe valid on November 11, 2013 at 03:00 UTC

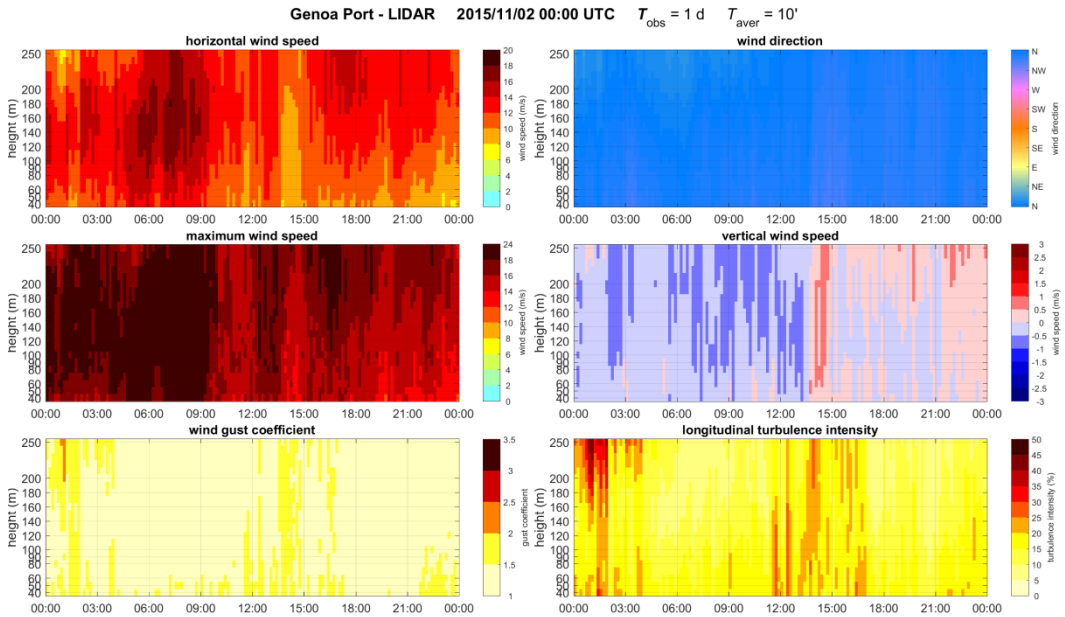

Fig. 10 Wind velocity field measured on November 2, 2015 (time in UTC) by the LiDAR in the Port of Genoa. The diagrams show the evolution of the vertical wind profiles with respect to time: 10-minute averaged horizontal wind speed (top left) and direction (top right), peak wind speed (centre left), vertical wind speed (centre right), gust factor (bottom left), and longitudinal turbulence intensity (bottom right)

This downslope wind event, which has been measured by the LiDAR installed in the Western part of the Port of Genoa, caused serious local problems to port activities and navigation. Fig. 10 shows the measurements of mean wind speed and turbulence properties recorded by the LiDAR on November 2, 2015. During all the day, the LiDAR recorded a wind blowing from North all along the vertical profile up to 250 m AGL (top right panel in Fig. 10). Early in the morning, between 5:00 and 9:00 UTC, the mean wind speed increased up to about 20 m/s in a layer between 100 and 200 m AGL (top left panel), with peak wind speed up to 24 m/s (centre left panel; here the peak wind speed conventionally coincides with the maximum value since the LiDAR sampling rate is 1 Hz) that determined values of the gust factor between 1 and 1.5, slightly higher at the measurement levels closer to the ground (bottom left panel), and turbulence intensity values not larger than 20% (bottom right panel). The vertical wind speed (centre right panel) is lower than 0 all the morning until midday, according to the prevailing downward gravitational flow along the valley, positive at 14-15 UTC and neutral afterwards, when convection driven by diurnal solar heating increases.

Fig. 11 shows the details of the measurements recorded by the LiDAR in the 10-minute time interval between 06:50 and 07:00 UTC, in terms of vertical mean wind profiles (top left), turbulence (top right), wind directions (bottom left), gust factors and Gaussianity (bottom right). The vertical mean profile presents a nose-like shape with maximum at 120 m AGL, and slightly negative average vertical components. This is consistent with the conceptual model of katabatic flow, reported for example by Poulos *et al*. (2000), where the low-level jet structure is due to the

combination of a gravitational flow with the surface drag. Turbulence intensity profiles have slightly larger values closer to the ground, according to fluctuations of wider amplitude below approximately 90 m (see the black open circles in the top left panel). Gust factors seem to be roughly constant above (about 1.2) and below (about 1.4) 80 m. For each measuring height, the wind varies to a large extent according to a normal distribution, as confirmed by skewness and excess kurtosis values rather close to 0.

It is rather questionable and debated whether LiDAR can be used to measure turbulence. Several studies have shown that the turbulence intensity measured by cup anemometers differs to a certain extent from that of LiDARs (Wagner *et al*. 2009, IEA, 2013), depending on stability atmospheric conditions, measuring height, LiDAR type and the methodology to calculate variance and covariance.

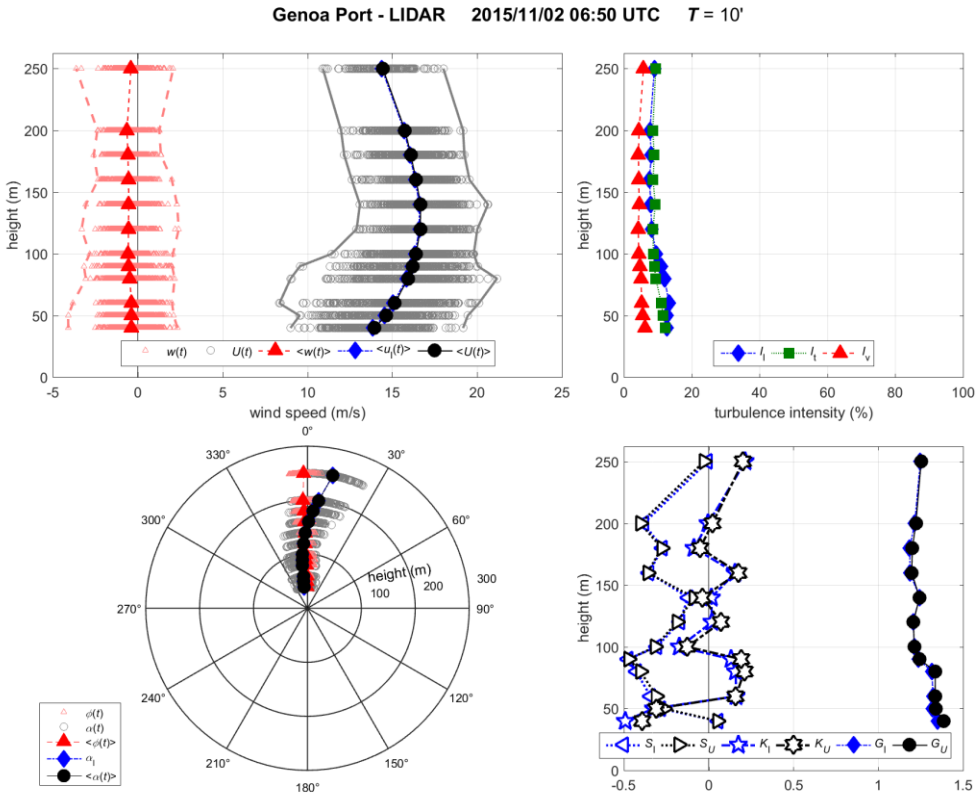

Fig. 11 Wind velocity field measured on November 2, 2015 at 6:50-7:00 UTC by the LiDAR in the Port of Genoa: profiles of 10-minute mean horizontal (<*U*>, circles), longitudinal (<u_l>, diamonds), and vertical (<*w*>, triangles) wind components and their variability up to 250 m above ground (top left); longitudinal, I_l, transversal, I_t, and vertical, I_v, turbulence intensities (top right); directions of the 10-minute mean horizontal (<α>, circles), longitudinal (α_l, diamonds), and vertical (ϕ, triangles) wind components and their variability as a function of height (bottom left); skewness, *S*, excess kurtosis, *K*, and gust factors, *G*, of the longitudinal (subscript *l*) and mean (subscript *U*) components (bottom right)

According to the model proposed by Sathe *et al*. (2011), not negligible systematic errors for the vertical and horizontal velocity variance can occur depending on the atmospheric stability conditions. Frehlich and Kelley (2008), however, concluded that careful corrections for the spatial filtering of the wind field operated by LiDARs can be applied to obtain turbulence estimates equivalent to point sensors. In the present paper, turbulence intensities have been evaluated without any correction. The exact quantitative evaluation of possible systematic errors in this kind of measurements is beyond the scope of this paper. The reader, however, is advised that turbulence estimations by LiDAR have to be interpreted in qualitative terms only.

In the meanwhile, authors plan to collect systematically other vertical wind profiles detected by LiDAR to make this discussion more robust and to classify and interpret different types of downslope wind flows.

5. Conclusions

Downslope winds in Liguria can be driven by different meteorological conditions that have not been analysed systematically yet. The wind monitoring network of the projects WP and WPS make available quite long-term measurements that can be used to investigate experimentally these phenomena for the first time. In this paper, firstly the wind climatology of strong slope winds in Liguria is presented for a valley located in between Alps and Apennines. Then, two selected events have been analysed in order to describe the main characteristics of intense downslope winds.

From the climatological analysis reported in Section 3, a precise seasonal collocation of the strong downslope windstorms that occurred from the end of October 2011 for 4 years in the Port of Vado Ligure has been obtained, and the general characteristics of such events in terms of mean and peak wind speeds, direction, turbulence and gustiness has been presented. Several issues, however, deserve further studies, in particular the directional distribution of the extreme wind speed, the harmonic content of turbulent fluctuations in different wind conditions, the large variability of the longitudinal turbulence intensity and gust factor even in presence of strong wind intensities, the separation and classification of downslope wind events associated with different meteorological conditions.

The first event considered in Section 4, which occurred in November 2013 in Vado Ligure, was the strongest recorded during the 4-year period mentioned above, with maxima higher than 30 m/s and gust factors larger than 2. Moreover, a pulsation at the time scale of 11 minutes has been detected, which has been already reported in literature for Bora events in the Dinaric Alps. This could suggest a common mechanism to sustain gustiness that will be studied in the next future. The second event considered occurred in November 2015 in Genoa. Here, a LiDAR belonging to the WP monitoring network is available that allowed to characterise the whole vertical wind profile of this phenomenon. In particular, a nose-shaped profile has been measured that, together with the analysis of the synoptic and local meteorological conditions, seems to support the idea that most downslope windstorms in Liguria are actually gap flows. It is not clear, however, to what extent this hypothesis may be generalised and further analysis will be soon performed considering a greater number of test-cases to clarify this point.

The results reported in this paper can be regarded as a rational framework to develop, on the one hand, new investigations aiming to improve the knowledge of downslope wind flows, for instance inspecting the issues discussed above, and, on the other hand, to inspect a broad band of wind engineering problems related to mountain conditions on more robust bases. Kozmar *et al*.

(2015), for example, have recently analysed the role of crosswind bora gusts as a possible cause of vehicles overturning or collision over bridges. The Ligurian highway, which crosses entirely the Alps and Apennines from the Western to the Eastern edge of the Region, has more than 150 tunnels and many bridges and viaducts where strong dangerous downslope winds often occur that give rise to many accidents. In Liguria and in several other Italian and foreign regions strong downslope winds affect port activities, also, causing conditions ranging from interrupting activities to produce several damage and fatalities. All the products, i.e., forecast systems and monitoring equipment, developed in the framework of projects WP and WPS (Solari *et al*. 2012, Burlando *et al.* 2015) were thought to be a valuable support to the port operations and navigation, indeed. Besides, at present, the authors are working on developing new numerical strategies to simulate and forecast strong downslope winds in the urban areas. Finally, the information about the wind profiles measured by the LiDAR in Genoa will become soon available to the Airport of Genoa, which is located inside the port area and whose glide paths intersect the flow at the exit of the Turchino Valley.

Acknowledgements

Anemometric data have been recorded by the wind monitoring network of the European Projects "Wind and Ports" and "Wind, Ports, and Sea", funded by the Cross-border Cooperation Programme "Italy-France Maritime 2007-2013". Authors thankfully acknowledge the cooperation of the Port Authorities of Genoa, La Spezia, Livorno, Savona and Bastia. Satellite images are based on Level 1 Data recorded by SEVIRI instrument on board Meteosat Second Generation satellites, operated by EUMETSAT. This research has been carried out in the framework of the Project "Wind monitoring, simulation and forecasting for the smart management and safety of port, urban and territorial systems", financed by Compagnia di San Paolo.

References

Barry, R.G. (1992), *Mountain Weather and Climate - 2nd Ed.*, Routledge Publishing Company, London and New York.

Bastin, S. and Drobinski, P. (2005), "Temperature and wind velocity oscillations along a gentle slope during sea-breeze events", *Bound. – Lay. Meteorol.*, **114**, 573-594.

Belusic, D., Pasaric, M. and Orlic, M. (2004), "Quasi-periodic bora gusts related to the structure of the troposphere", *Q. J. Roy. Meteorol. Soc.*, **130**, 1103-1121.

Belusic, D., Zagar, M. and Grisogono, B. (2007), "Numerical simulation of pulsations in the bora wind", *Q. J. Roy. Meteorol. Soc.*, **133**, 1371-1388.

Bond, N.A., Dierking, C.F. and Doyle, J.D. (2006), "Research Aricraft and Wind Profiler Observations in Gastineau Channel during a Taku Wind Event", *Weather Forecast.*, **21**, 489-501.

Bougeault, P., Blinder, P., Buzzi, A., Dirks, R., Houze, R.A., Kuettner, J., Smith, R.B., Steinacker, R. and Volkert, H. (2001), "The MAP special observing period", *Bull. Am. Meteorol. Soc.*, **82**, 433-462.

Burlando, M., De Gaetano, P., Pizzo, M., Repetto, M.P., Solari, G. and Tizzi, M. (2013), "Wind climate analysis in complex terrains", *J. Wind Eng. Ind. Aerod.*, **123**, 349-362.

Burlando, M., De Gaetano, P., Pizzo, M., Repetto, M.P., Solari, G., Tizzi, M. and Bonino, G. (2015), "The European project Wind, Ports, and Sea", *Proceedings of the 14th International Conference on Wind Engineering*, June 21-26, Porto Alegre, Brasil.

Castino, F., Rusca, L. and Solari, G. (2003), "Wind climate micro-zoning: a pilot application to Liguria Region (North Western Italy)", *J. Wind Eng. Ind. Aerod.*, **91**, 1353-1375.
Chen, X. and Huang, G. (2010), "Estimation of probabilistic extreme wind load effects: combination of aerodynamic and wind climate data", *J. Eng. Mech. - ASCE*, **136**, 747-760.
Clark, T.L. and Peltier, W.R. (1977), "On the evolution and stability of finite-amplitude mountain waves", *J. Atmos. Sci.*, **34**, 1715-1730.
CNR-DT 207/2008 (2010), *Guide for the assessment of wind actions and effects on structures*, National Research Council, Rome, Italy.
Corby, G.A. (1954), "The airflow over mountains - A review of the state of current knowledge", *Q. J. Roy. Meteorol. Soc.*, **80**, 491-521.
De Gaetano, P., Repetto, M.P., Repetto, T. and Solari, G. (2014), "Separation and classification of extreme wind events from anemometric records", *J. Wind Eng. Ind. Aerod.*, **126**, 132-143.
Defant, F. (1951), "Local winds", in *Compendium of Meteorology*, American Meteorological Society, Boston, Massachusetts, 655-672.
Doran, J.C. and Horst, T.W. (1981), "Velocity and temperature oscillations in drainage winds", *J. Appl. Meteorol.*, **20**, 361-364.
Durran, D.R. (1990), "Mountain waves and downslope winds", in *Atmospheric Processes Over Complex Terrain*, W. Blumen (Ed.), Meteorological Monograph, **23**(45), *Am. Meteorol. Soc.*, Boston, Massachusetts, 59-81.
Engineering Sciences Data Unit (1993), "*Computer program for wind speeds and turbulence properties: flat or hill sites in terrain with roughness changes*", ESDU Item 92032, London, U.K.
EUMETSAT (2013) "MTG-FCI: ATBD for Cloud Mask and Cloud Analysis Product", *Technical Report* EUM/MTG/DOC/10/0542, Eumetsat.
Eurocode 1 (2005) *Actions on structures – General actions. Part 1-4: Wind actions*, CEN, EN 1991-1-4:2005
Fleagle, R.G. (1950), "A theory of air drainage", *J. Meteor.*, **7**, 227-232.
Frehlich, R. and Kelley, N. (2008), "Measurements of wind and turbulence profiles with scanning doppler lidar for wind energy applications", *IEEE Journal of Selected Topics in Applied Earth Observations and Remote Sensing*, **1**(1), 42-47.
Gomes, L. and Vickery, B.J. (1977), "On the prediction of extreme wind speed from the parent distribution", *J Wind Eng. Ind. Aerod.*, **2**, 21-36.
Gomes, L. and Vickery, B.J. (1977, 1978), "Extreme wind speeds in mixed climates", *J. Ind. Aerod.*, **2**, 331-344.
Grubisic, V. and Lewis, J.M. (2004), "Sierra Wave Project Revisited: 50 Years Later", *Bull. Am. Meteorol. Soc.*, **85**, 1127-1142.
Gumbel, E.J. (1954), *Statistical theory of extreme values and some practical applications*, Applied Mathematics Series 33 (1st Ed.), U.S. Department of Commerce, National Bureau of Standards.
Harris, R.I. and Cook, N.J. (2014), "The parent wind speed distribution: Why Weibull?", *J. Wind Eng. Ind. Aerod.*, **131**, 72-87.
Hoaglin, D.C., Mostaller, F. and Tukey, J.W. (1983), *Understanding robust and exploratory data analysis*, Wiley, New York.
IEA (2013), "Ground-based vertically-profiling remote sensing for wind resource assessment", *Technical Report* IEA Wind RP 15, International Energy Agency.
Kareem, A. (1990), "Reliability analysis of wind-sensitive structures", *J. Wind Eng. Ind. Aerod.*, **33**, 495-514.
Klemp, J.B. and Lilly, D.K. (1975), "The dynamics of wave-induced downslope winds", *J. Atmos. Sci.*, **32**, 320-339.
Kozmar, H., Butler, K. and Kareem, A. (2015), "Downslope gusty wind loading of vehicles on bridges", *J. Bridge Eng.*, **20**(11), 04015008.
Kruger, A.C., Goliger, A.M., Retief, J.V. and Sekele, S.S. (2012), "Clustering of extreme winds in the mixed climate of South Africa", *Wind Struct.*, **15**(2), 87-109.
Kwon, S.D. (2009), "Uncertainty analysis of wind energy potential assessment", *Appl. Energy*, **87**, 856-865.

Lagomarsino, S., Piccardo, G. and Solari, G. (1992), "Statistical analysis of high return period wind speeds", *J. Wind Eng. Ind. Aerod.*, **41**, 485-496.
Lee, T.J., Pielke, R.A., Kessler, R.C. and Weaver, J. (1989), "Influence of Cold Pools Downstream of Mountain Barriers on Downslope Winds and Flushing", *Mon. Weather. Rev.*, **117**, 2041-2058.
Lilly, D.K. (1978), "A severe downslope windstorm and aircraft turbulence event induced by a mountain wave", *J. Atmos. Sci.*, **35**, 59-77.
Lilly, D.K. and Zipser, E.J. (1972), "The front range windstorm of 11 January 1972 - a meteorological narrative", *Weatherwise*, **25**, 56-63.
Lombardo, F.T., Main, J.A. and Simiu, E. (2009), "Automated extraction and classification of thunderstorm and non-thunderstorm wind data for extreme-value analysis", *J. Wind Eng. Ind. Aerod.*, **97**, 120-131.
Lu, H.C. and Fang, G.C. (2002), "Estimating the frequency distributions of PM_{10} and $PM_{2.5}$ by the statistics of wind speed at Sha-Lu, Taiwan", *Sci. Total Environ.*, **298**, 119-130.
Meyers, M.P., Snook, J.S., Wesley, D.A. and Poulos, G.S. (2003), "A rocky mountain storm. Part II: The forest blowdown over the west slope of the northern colorado mountains – observations, analysis, and modeling", *Weather Forecast.*, **18**, 662-674.
Neiman, P.J., Hardesty, R.M., Shapiro, M.A. and Cupp, R.E. (1988), "Doppler lidar observations of a downslope windstorm", *Mon. Weather Rev.*, **116**, 2265-2275.
NWC SAF (2013) "Algorithm Theoretical Basis Document for Cloud Products", *Technical Report* SAF/NWC/CDOP2/MFL/SCI/ATBD/01, NWC SAF, Meteo France.
Pagnini, L.C. and Solari, G. (1998), "Serviceability criteria for wind-induced acceleration and damping uncertainties", *J. Wind Eng. Ind. Aerod*., **74-76**, 1067-1078.
Pagnini, L.C., Burlando, M. and Repetto, M.P. (2015), "Experimental power curve of small-size wind turbines in turbulent urban environment", *Appl. Energy*, **154**, 112-121.
Peltier, W.R. and Clark, T.L. (1979), "On the evolution and stability of finite-amplitude mountain waves. Part II: surface wave drag and severe downslope windstorms", *J. Atmos. Sci.*, **36**, 1498-1529.
Pena, A., Hasager, C.B., Gryning, S.E., Courtney, M., Antoniou, I., Mikkelsen, T. (2009), "Offshore wind profiling using light detection and ranging measurements", *Wind Energy*, **12**, 105-124.
Poulos, G.S., Bossert, J.E., McKee, T.B. and Pielke, R.A. (2000), "The interaction of Katabatic flow and mountain waves. Part I: observations and idealized simulations", *J. Atmos. Sci.*, **57**, 1919-1936.
Princevac, M., Hunt, J.C.R. and Fernando, H.J.S. (2008), "Quasi-steady Katabatic winds on slopes in wide valleys: Hydraulic theory and observations", *J. Atmos. Sci.*, **65**,627-643.
Repetto, M.P. and Solari, G. (2010), "Wind-induced fatigue collapse of real slender structures", *Eng. Struct.*, **32**, 3888-3898.
Romanić, D., Ćurić, M., Lompar, M. and Jovičić, I. (2016a), "Contributing factors to Koshava wind characteristics", *Int. J. Climatol.*, **36**, 956-973.
Romanić, D., Ćurić, M., Zarić, M., Lompar, M. and Jovičić, I. (2016b), "Investigation of an extreme Koshava wind episode of 30 January–4 February 2014", *Atmos. Sci. Lett.*, **17**, 199-206.
Sathe, A. and Mann, J. (2013), "A review of turbulence measurements using ground-based wind lidars", *Atmos. Meas. Tech.*, **6**, 3147-3167.
Sathe, A., Mann, J., Gottschall, J. and Courtney, M.S. (2011), "Can wind lidars measure turbulence?", *J. Atmos. Oceanic Technol.*, **28**, 853-868.
Smith, D.A., Harris, M. and Coffey, A.S. (2006), "Wind Lidar evaluation at the Danish wind test site in Hovsore", *Wind Energy*, **9**, 87-93.
Smith, R.B. (1979), "The influence of mountains on the atmosphere", *Adv. Geophys.*, **21**, 87-230.
Smith, R.B. (1985), "On severe downslope winds", *J. Atmos. Sci.*, **42**(23), 2597-2603.
Smith, R.B. (1987), "Aerial observations of the Yugoslavian Bora", *J. Atmos. Sci.*, **44**(2), 269-297.
Smith, R.B., Doyle, J.D., Jiang, Q. and Smith, S.A. (2007), "Alpine gravity waves: Lessons from MAP regarding mountain wave generation and breaking", *Q. J. Roy. Meteorol. Soc.*, **133**, 917-936.
Solari, G. (1993), "Gust buffeting. I: peak wind velocity and equivalent pressure", *J. Struct. Eng.- ASCE*, **119**, 365-382.
Solari, G. (1996a), "Wind speed statistic", in *Modelling of Atmospheric Flow Fields*, (Eds., Lalas D.P. and

Ratto C.F.), World Scientific, Singapore.
Solari, G. (1996b), "Statistical analysis of extreme wind speeds", in *Modelling of atmospheric flow fields*, (Eds., Lalas D.P. and Ratto C.F.), World Scientific, Singapore.
Solari, G. (2014), "Emerging issues and new frameworks for wind loading on structures in mixed climates", *Wind Struct.*, **19**(3), 295-320.
Solari, G., Burlando, M., De Gaetano, P., Repetto, M.P. (2015), "Characteristics of thunderstorms relevant to the wind loading of structures", *Wind Struct.*, **20**(6), 763-791.
Solari, G., Repetto, M.P., Burlando, M., De Gaetano, P., Pizzo, M., Tizzi, M. and Parodi, M. (2012), "The wind forecast for safety management of port areas", *J. Wind Eng. Ind. Aerodyn.*, **104-106**, 266-277.
Sterling, M., Baker, C.J., Richards, P.J., Hoxey, R.P., Quinn, A.D. (2006), "An investigation of the wind statistics and extreme gust events at a rural site", *Wind Struct.*, **9**(3), 193-215.
Takle, E.S., Brown, J.M. (1978), "Note on the use of Weibull statistics to characterize wind speed data", J. Appl. Meteorol., **17**, 556–559.
Torrielli, A., Repetto, M.P. and Solari, G. (2013), "Extreme wind speeds from long-term synthetic records", *J. Wind Eng. Ind. Aerod.*, **115**, 22-38.
Torrielli, A., Repetto, M.P. and Solari, G. (2014). "A refined analysis and simulation of the wind speed macro-meteorological components", *J. Wind Eng. Ind. Aerod.*, **132**, 54-65.
Trigo, I.F., Bigg, G.R. and Davies, T.D. (2002), "Climatology of cyclogenesis mechanisms in the mediterranean", *Mon. Weather. Rev.*, **130**, 549-569.
Wagner, R., Mikkelsen, T. and Courtney, M. (2009), "Investigation of turbulence measurements with a continuous wave, conically scanning Lidar", *Technical Report* Risø-R-1682(EN), Risø National Laboratory for Sustainable Energy, Technical University of Denmark, Roskilde, Denmark.
Weibull, W. (1951), "A statistical distribution function of wide applicability", *J. Appl. Mech.*, **18**, 293-297.
Whiteman, C.D. (2000), *Mountain Meteorology: Fundamentals and Applications*, Oxford University Press, New York.
Whiteman, C.D. and Zhong, S. (2008), "Downslope flows on a low-angle slope and their interactions with valley inversions. Part I: observations", *J. Appl. Meteorol. Clim.*, **47**, 2023-2038.
Wilczak, J.M., Gossard, E.E., Neff, W.D. and Eberhard, W.L. (1996), "Ground-based remote sensing of the atmospheric boundary layer: 25 years of progress", *Bound. - Lay. Meteorol.*, **78**, 321-349.
Xu, Q., Gao, S. and Fiedler, B.H. (1996), "A theoretical study of cold air damming with upstream cold air flow", *J. Atmos. Sci.*, **53**(2), 312-326.
Zangl, G. (2002), "Stratified flow over a mountain with a gap: Linear theory and numerical simulations", *Q. J. Roy. Meteorol. Soc.*, **128**, 927-949.